ADVANCED FUNCTIONAL MATERIALS

Supporting Information

for *Adv. Funct. Mater.*, DOI: 10.1002/adfm.201701832

Nanogap-Rich Au Nanowire SERS Sensor for Ultrasensitive Telomerase Activity Detection: Application to Gastric and Breast Cancer Tissues Diagnosis

Gayoung Eom, Hongki Kim, Ahreum Hwang, Hye-Young Son, Yuna Choi, Jeong Moon, Donghyeong Kim, Miyeon Lee, Eun-Kyung Lim, Jinyoung Jeong, Yong-Min Huh, Min-Kyo Seo, Taejoon Kang, and Bongsoo Kim**

Supporting Information

Nanogap-Rich Au Nanowire SERS Sensor for Ultrasensitive Telomerase Activity Detection: Application to Gastric and Breast Cancer Tissues Diagnosis

Gayoung Eom, Hongki Kim, Ahreum Hwang, Hye-Young Son, Yuna Choi, Jeong Moon, Donghyeong Kim, Miyeon Lee, Eun-Kyung Lim, Jinyoung Jeong, Yong-Min Huh, Min-Kyo Seo, Taejoon Kang, and Bongsoo Kim**

1. SEM images of Au NWs grown on a sapphire substrate

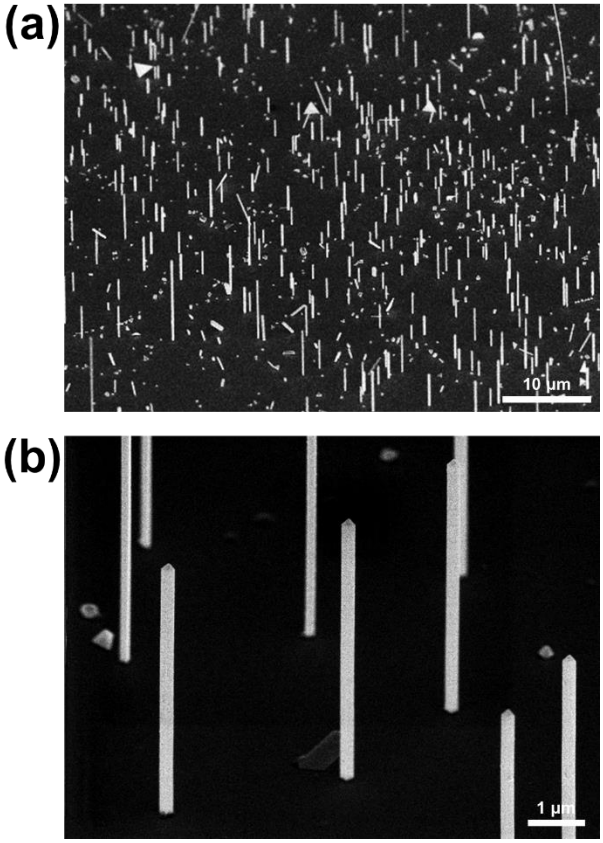

Figure S1. (a) SEM image of Au NWs grown on a sapphire substrate. (b) Magnified SEM image of (a).

2. SERS spectra of MB measured from nanogap-rich Au NW SERS sensors with various sputtering time

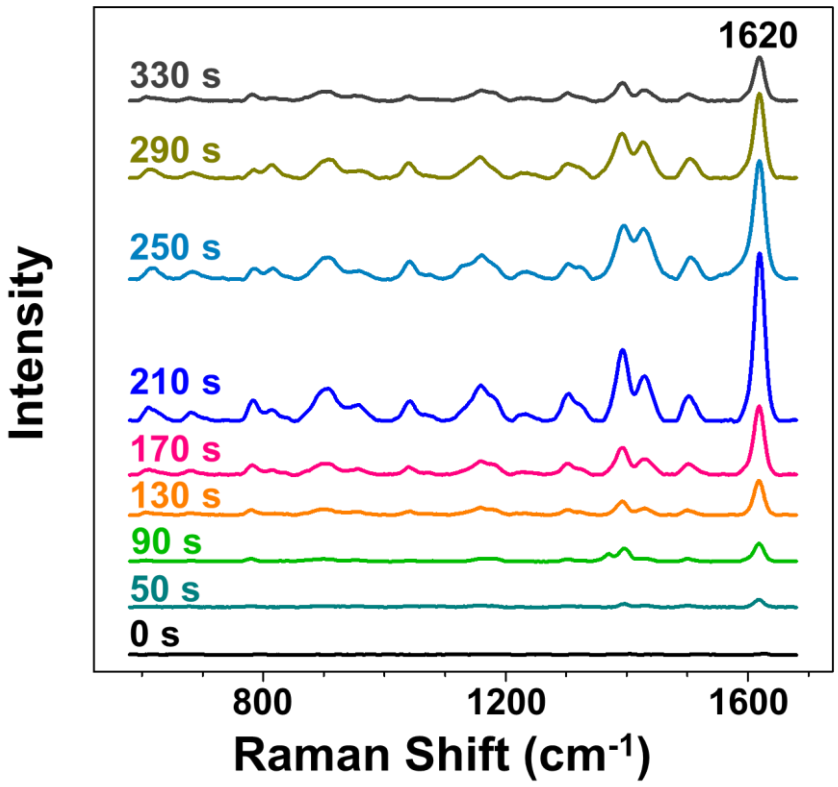

Figure S2. SERS spectra of MB measured from nanogap-rich Au NW SERS sensors with sputtering time of 0, 50, 90, 130, 170, 210, 250, 290, and 330 s.

3. Diameter of NPs and gap size on nanogap-rich Au NWs with various sputtering time

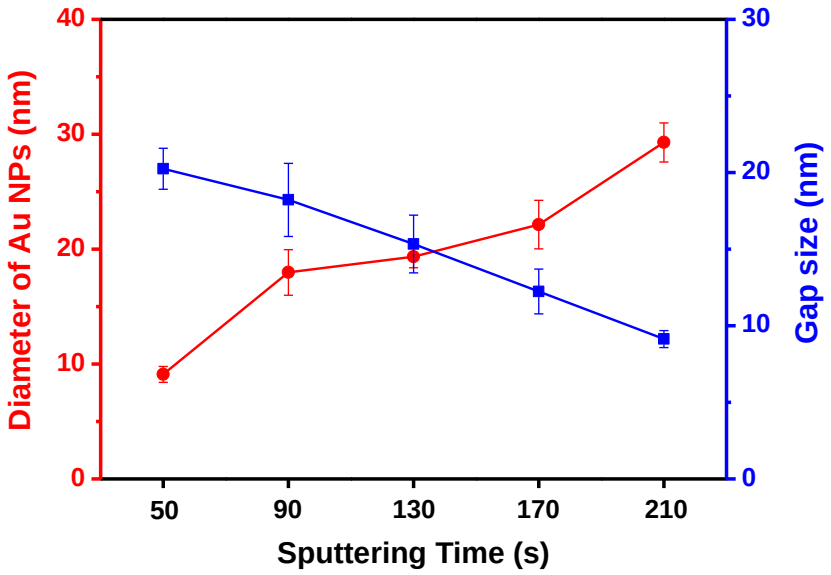

Figure S3. Diameter of Au NPs (Red) and gap size (Blue) on nanogap-rich Au NW SERS sensors plotted as a function of sputtering time. Data represents the average plus standard deviation from 3 measurements.

4. SERS spectra of MB obtained from nanogap-rich Au NW SERS sensor and various substrates

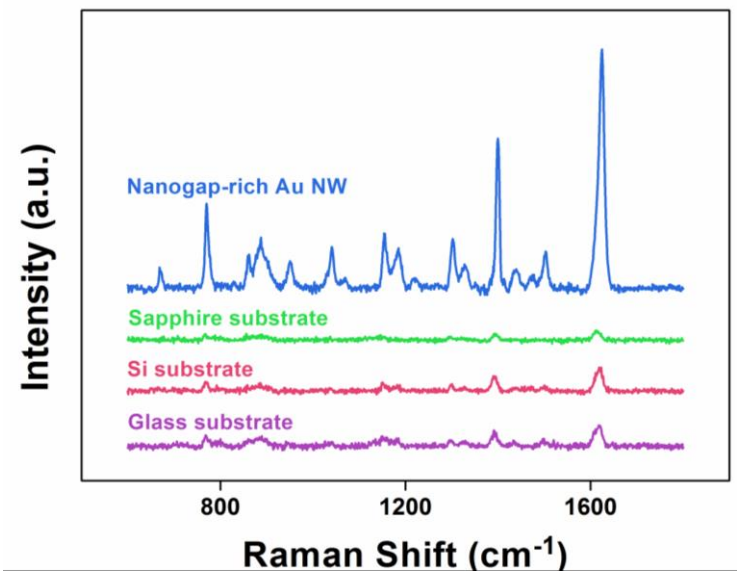

Figure S4. SERS spectra of MB obtained from nanogap-rich Au NW (Blue spectrum), sapphire (Green spectrum), Si (Pink spectrum), and glass substrates (Purple spectrum) after sputtering of Au NPs. All samples were prepared at the sputtering time of 210 s.

5. EF of nanogap-rich Au NW SERS sensor

To calculate the EF of nanogap-rich Au NW SERS sensor, we obtained SERS and Raman spectra of MB from a nanogap-rich Au NW SERS sensor and a glass, respectively. We calculated EF of nanogap-rich Au NW SERS sensor using the expression of EF = $(I_{SERS}/I_{Ref}) \times (N_{Ref}/N_{SERS})$. I_{SERS} is the intensity of 1620 cm^{-1} MB band on a nanogap-rich Au NW SERS sensor and I_{Ref} is the intensity of 1620 cm^{-1} MB band on a glass. N_{SERS} is the number of MB molecules contributing to I_{SERS} and N_{Ref} is the number of MB molecules contributing to I_{Ref}. Assuming the uniform adsorption of MB molecules, the expression can be changed to EF = $(I_{SERS}/I_{Ref}) \times (A_{Ref}/A_{SERS})$. A_{SERS} is the surface area of SERS-active region in the nanogap-rich Au NW SERS sensor and A_{Ref} is the laser-illuminated area of a glass. The diameter of nangap-rich Au NW is 200 nm and A_{SERS} is caculated to be 5.65×10^5 nm^2. The diameter of laser spot is 1 μm and A_{Ref} is calculated to be 7.85×10^5 nm^2. Therefore, the EF of nanogap-rich Au NW SERS sensor was calculated to be 1.34×10^4.

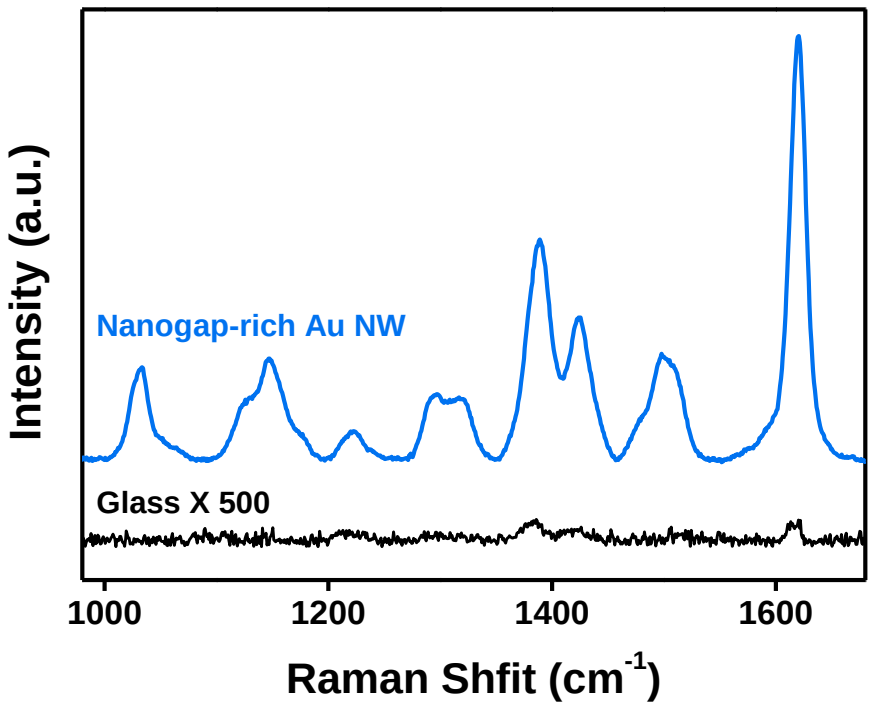

Figure S5. SERS and Raman spectra of MB from nanogap-rich Au NW SERS sensor (Blue spectrum) and glass (Black spectrum), respectively. Spectrum from glass is 500-fold magnified in the vertical scale.

6. Distribution of electric field over nanogap-rich Au NW SERS sensor

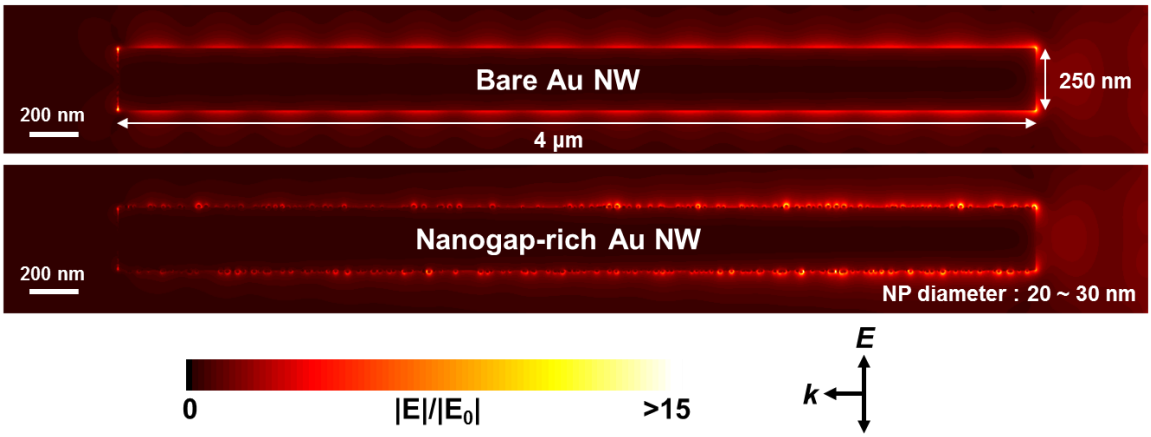

Figure S6. Distribution of electric field over bare Au NW and nanogap-rich Au NW SERS sensor. The wavelength of excitation light is 633 nm. The *k*- and *E*-vectors indicate the incident direction and the polarization direction of light, respectively.

7. Optimization of telomerase reaction time

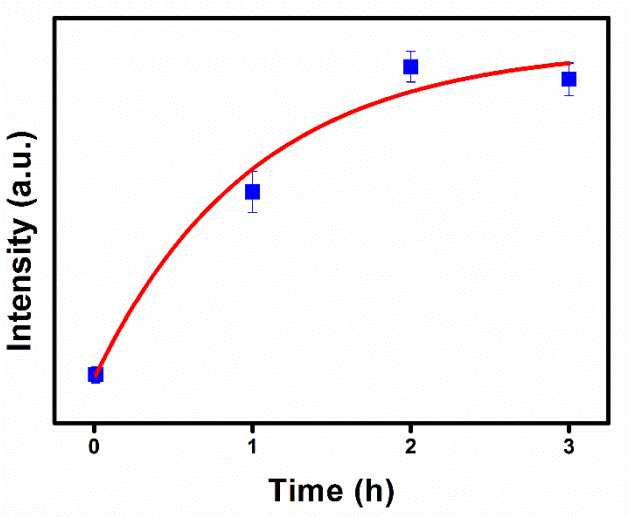

Figure S7. Intensity of MB 1620 cm^{-1} band plotted as a telomerase reaction time. HeLa cell concentration was 10^4 cells/mL. Red curve indicates the exponentially fitted curve. Data represent the average plus standard deviation from 7 measurements.

8. SERS spectra of MB measured from nanogap-rich Au NW SERS sensors at various HeLa cell concentrations

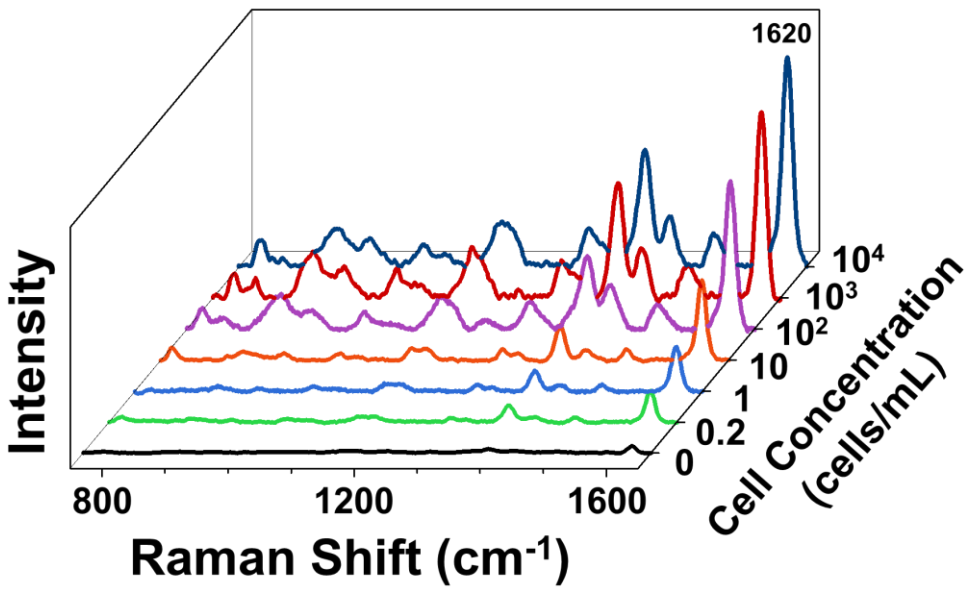

Figure S8. SERS spectra of MB measured from nanogap-rich Au NW SERS sensors at various HeLa cell concentrations of 0, 0.2, 1, 10, 10^2, 10^3, and 10^4 cells/mL.

9. SERS spectra of MB measured from nanogap-rich Au NW SERS sensors in various cell lines

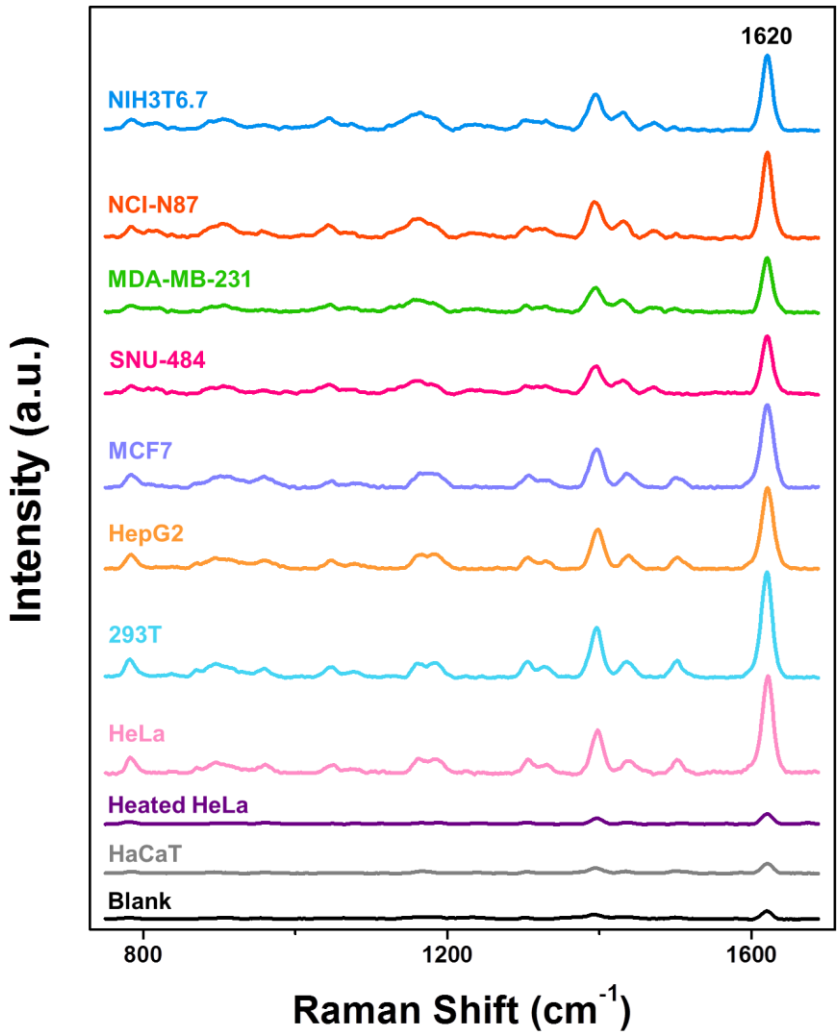

Figure S9. SERS spectra of MB measured from nanogap-rich Au NW SERS sensors in blank, heated HeLa, and various cell line samples (HaCaT, HeLa, 293T, HepG2, MCF7, SNU-484, MDA-MB-231, NCI-N87, and NIH3T6.7). All samples are in 10 cells/mL concentration.

10. SERS spectra of MB in tumor, heated tumor, and normal tissues from 16 tumor-bearing mice

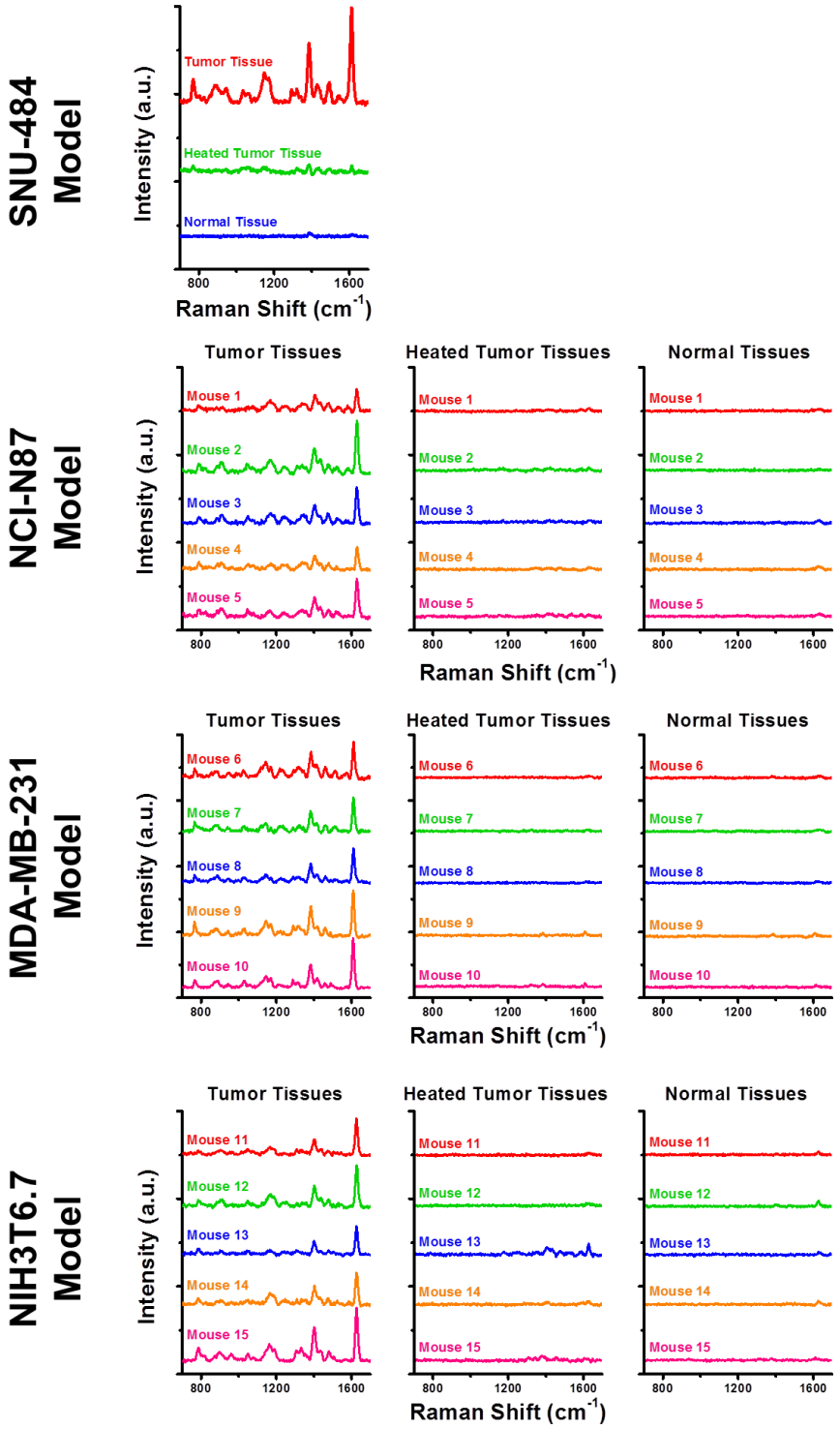

Figure S10. SERS spectra of MB in tumor, heated tumor, and normal tissues excised from SNU-484 (n=1), NCI-N87 (n=5), MDA-MB-231 (n=5) and NIH3T6.7 models (n=5).

11. SERS spectra of MB in various organ tissues excised from SNU-484 model and normal mouse

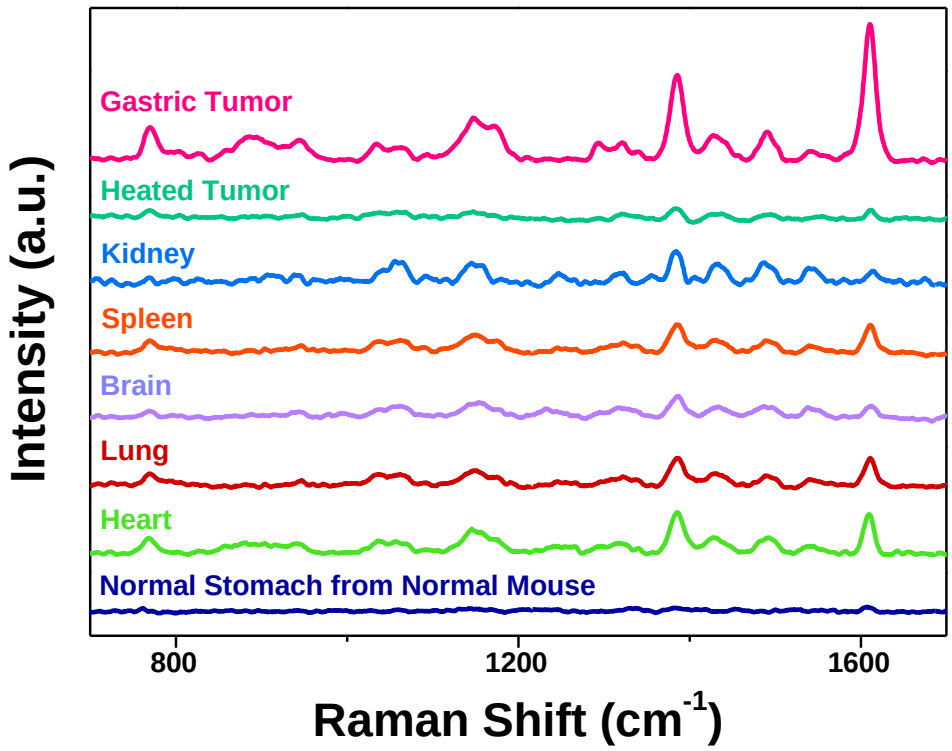

Figure S11. SERS spectra of MB in various organ tissues (gastric tumor, heated tumor, kidney, spleen, brain, lung, heart, and normal stomach tissues) excised from SNU-484 model and normal mouse.

12. SERS spectra of MB in various organ tissues excised from NCI-N87, MDA-MB-231 and NIH3T6.7 models

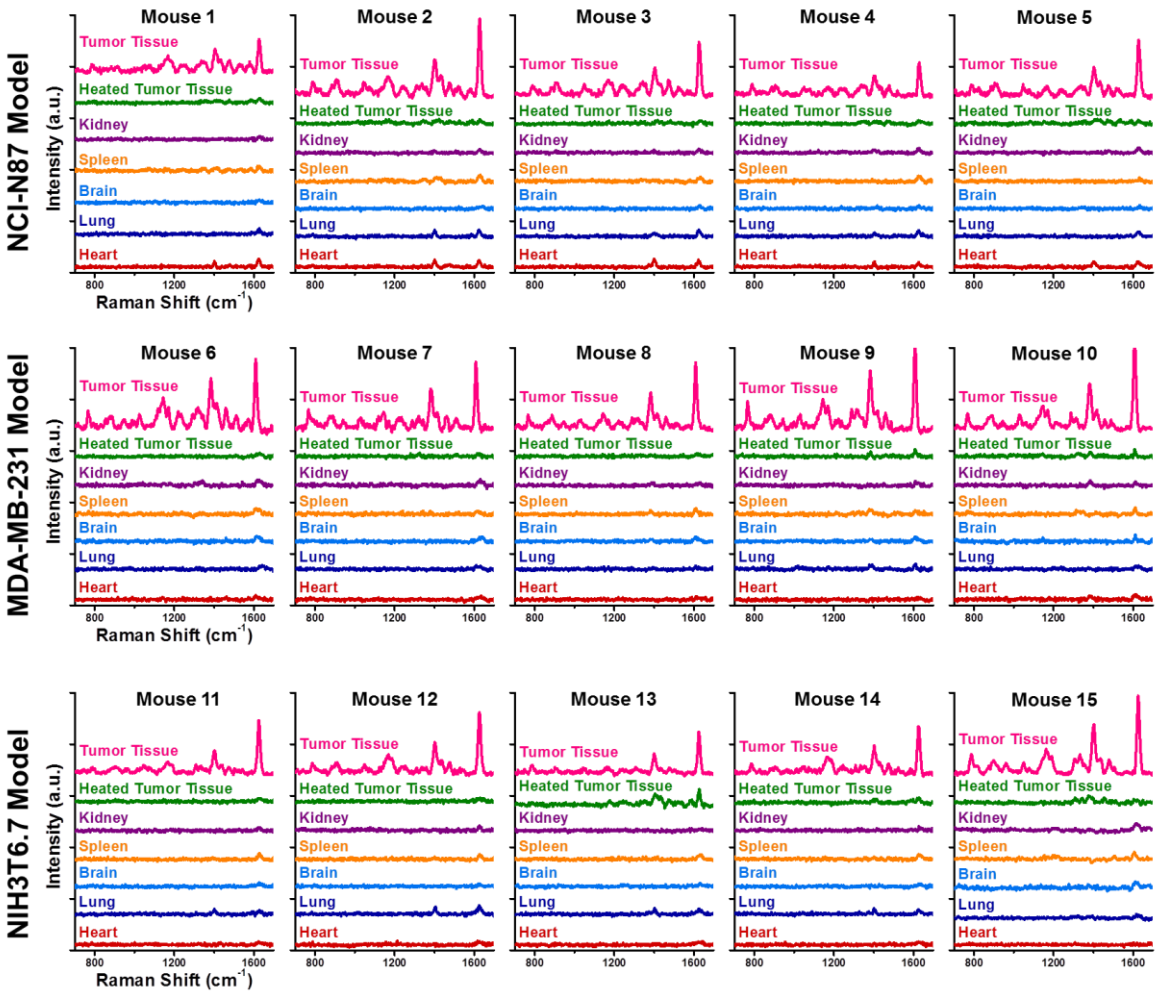

Figure S12. SERS spectra of MB in various organ tissues (tumor, heated tumor, kidney, spleen, brain, lung, and heart) excised from NCI-N87 (n=5), MDA-MB-231 (n=5), and NIH3T6.7 models (n=5).